J Mater Sci: Mater Med (2011) 22:2347–2356
DOI 10.1007/s10856-011-4401-9

Bone marrow stromal cells-loaded chitosan conduits promote repair of complete transection injury in rat spinal cord

Xue Chen · Yang Yang · Jian Yao · Weiwei Lin · Yi Li · Ying Chen · Yilu Gao · Yumin Yang · Xiaosong Gu · Xiaodong Wang

Received: 18 December 2010 / Accepted: 14 July 2011 / Published online: 28 July 2011

Abstract In this study, a chitosan conduit loaded with bone marrow stromal cells (BMSCs) was developed to bridge the gap in the transected spinal cord of adult rats, and the nerve repair outcomes were evaluated by functional and histological techniques at 12 weeks after implantation. As compared to chitosan conduits alone, incorporation of BMSCs within chitosan conduits yielded additional improving effects on nerve regeneration and function restoration. The measurements with the Basso, Beattie and Bresnahan locomotor rating scale or of motor evoked potentials indicated that motor functional recovery was enhanced; retrograde tracing confirmed that the ascending tract was regenerated and the neural pathway was established; and histological analyses revealed that axon growth and remyelination in the regenerated nerve was promoted. The three-dimensional reconstruction showed that the chitosan conduit loaded with BMSCs significantly reduced the spinal cord cavity volume at the injured site. Taken together, the results collectively suggest that implantation with BMSCs-loaded chitosan conduits may become a promising approach to the repair of spinal cord injury.

Xue Chen and Yang Yang contributed equally to this work.

X. Chen · Y. Yang · J. Yao · W. Lin · Y. Li · Y. Chen · X. Wang (✉)
Department of Histology and Embryology, Medical College, Nantong University, Nantong 226001, Jiangsu, China
e-mail: wxdzw@ntu.edu.cn; wxdzw@hotmail.com

Y. Gao · X. Wang
Department of Neurosurgery, Affiliated Hospital of Nantong University, Nantong 226001, Jiangsu, China

Y. Yang · X. Gu · X. Wang
Jiangsu Key Laboratory of Neuroregeneration, Nantong University, Nantong 226001, Jiangsu, China

1 Introduction

Spinal cord injury (SCI) initiates a series of pathological events, including tissue loss, cell death and formation of cystic cavities and glial scars, thereby creating structural and environmental barriers to nerve regeneration and functional restoration [1]. An effective therapeutic strategy for SCI treatment requires not only neuron survival and axonal regeneration but also reconnection across the injury site in the spinal cord by bridging with grafts. Since autografts or allografts are associated with limited availability or immunological problems, tissue-engineered nerve grafts have been greatly developed for implantation in the injured spinal cord to promote nerve regeneration.

Tissue-engineered nerve grafts are usually composed of a nerve conduit filled with growth factors, extracellular matrices and/or cell implants. The nerve conduit that provides a structural support for axonal regeneration can be prepared with a variety of synthetic or natural biomaterials, among which chitosan is derived from chitin that is a naturally occurring polysaccharide composed of α-1, 4-linked *N*-acetyl-D-glucosamine. Chitosan has many desirable physicochemical and biological characteristics [2–4]. In vitro studies have indicated that chitosan is biocompatible to nerve cells and thus suitable for nerve regeneration [5, 6]. The greatest surface amine content and the lowest equilibrium water content of chitosan contribute to nerve cell survival, differentiation and growth [7]. In vivo, chitosan produces potent neuroprotection and physiological recovery following traumatic spinal cord injury and is degraded into chitooligosaccharides, which have been shown to possess nerve cell affinity by supporting nerve cell adhesion and promoting neuronal differentiation and neurite outgrowth [8, 9]. And moreover,

both chitosan and chitooligosaccharides have displayed their anti-oxidative activity [10].

On the other hand, the use of cell implants such as neural stem cells (NSCs) [11, 12], Schwann cells [13, 14] and olfactory ensheathing cells [15] has proven to enhance axonal regeneration within the peripheral and central nervous system. For instance, chitosan conduits loaded with NSCs were implanted into the lesion of spinal cord, achieving obvious functional recovery for the injured nerves [16].

Bone marrow stromal cells (BMSCs) are non-hematopoietic multipotent stem cells, and have transdifferentiation characteristics to give rise to astrocytes, oligodendrocytes, microglia, or neurons in vitro [17–20]. Recently, the promoting actions of BMSCs on nerve regeneration motivate the research interest of using these cells for SCI treatment [21, 22]. And it has been reported that BMSCs play a significant therapeutic role in an experimental model of paraplegia induced by severe SCI [23, 24].

Although the joint use of chitosan and BMSCs has been tried in the tissue engineering field for the generation of peripheral nerves [25], to our knowledge, there have been few reports about using chitosan in combination with BMSCs to repair SCI. Based on this, this study aimed to develop new nerve grafts which consisted of a chitosan conduit loaded with BMSCs, and investigate the feasibility of using these nerve grafts as a bridge for implantation in the completely transected spinal cord. The repair outcomes were evaluated at 12 weeks after implantation by a variety of functional tests, electrophysiological analysis and histological techniques.

2 Materials and methods

All experiments involving animals were approved ethically by the Administration Committee of Experimental Animals, Jiangsu Province, China, and conducted according to the guidelines of Institutional Animal Care and Use Committee, Nantong University.

2.1 Isolation and characterization of BMSCs

Bone marrow stromal cells (BMSCs) were isolated from the femur and tibias of adult Sprague–Dawley (SD) rats (180–200 g), followed by culture in Iscove's Modified Dulbecco's Medium (IMDM, GIBCO/BRL, Carlsbad, CA) supplemented with 20% fetal bovine serum (FBS) as previously described [26]. After the dissociated cells were incubated for 24 h, the non-adherent cells were removed, and the adherent cells were continuously cultured to 90% confluence, which were termed BMSCs at passage 0 and subjected to passage culture. BMSCs at passage 2 were characterized with different labeled monoclonal antibodies, including CD90-FITC, CD45-TRITC, and CD11b-PE (Sigma, St. Louis, MO), in dark at 4°C for 30 min, followed by phenotype analysis with a flow cytometer (BD FACScalibur, Franklin Lakes, NJ/San Jose, CA) as previously described [27].

2.2 Fabrication and characterization of chitosan conduits

The chitosan conduit was prepared by an injection molding process as previously described [28]. In brief, chitosan with a deacetylation degree of 92.3% and an average molecular weight of 2.2×10^4 D, provided by Xincheng Biochemical Company, Nantong, China, was dissolved in 2% acetic acid in a ratio of 1 g:20 ml, and stirred to form a white viscous liquid, followed by addition of the same weight of chitin (the acetylated form of chitosan). The resulting gel mixture was immediately injected into a stainless-steel casting mold. Then, the mold was immersed in a 20% sodium hydroxide solution for 4 h. Following rinse with double-distilled water to neutrality, demolding under lyophilization was performed to generate a chitosan conduit. The morphology of conduits was observed under scanning electron microscope (SEM) (JEM-T300, JEOL Ltd., Tokyo, Japan), and their structural parameters measured. The tensile strength or transverse compression strength of conduits was measured on a J-100N strength-testing machine under wet or dry conditions by making them be or be not soaked in phosphate buffered solution (pH 7.4) at 37°C. For measurement, the tensile speed and gauge length were set as 10 mm/min and 60 mm, respectively. The chitosan conduit was sterilized by ^{60}Co radiation prior to use.

2.3 Surgical procedures

SD rats, weighing 220–250 g, were anaesthetized by an intraperitoneal injection of 3% sodium pentobarbital solution (30 mg/kg body weight) before surgery. The spinal cord of animals was exposed at T8–T10 vertebra. A laminectomy was performed under an operation microscope. After the dura mater was cut, the spinal cord was incised about 2 mm from the level of T8 toward caudal end and completely removed, forming about 2 mm transection gap. The injury site was irrigated with normal saline, and bleeding was controlled using gelfoam.

The animals were randomly divided into three groups to receive different treatments. They were Chitosan group ($n = 15$), in which the transection gap in spinal cord was bridged by a chitosan conduit and the rostral and caudal stumps were inserted into the conduit without blood clot formation; BMSCs group ($n = 15$), in which the chitosan

conduit was implanted across the transaction gap in spinal cord as above mentioned, followed by injection of 10 μl of BMSCs suspension at passage 2 with the cell density of 10^8/ml into the conduit; and Unbridged group ($n = 10$), in which the transection gap in spinal cord was left untreated.

After surgery, the dura mater, muscle and skin were sutured. Then, all animals were subcutaneously injected with lactated Ringer's solution (10 ml/rat) to compensate for blood volume loss, placed to cages, and given easily accessible water and food at room temperature (24–26°C). To prevent urinary tract infection, penicillin (1×10^4 unit/kg) was administered daily during the first 7 days post-surgery. The bladder was massaged twice daily until the normal bladder function was restored.

2.4 Functional testing

The motor function was assessed by two observers blind to the treatment according to the Basso, Beattie and Bresnahan (BBB) locomotor rating scale [29, 30]. During post-surgery period, functional testing was performed thrice per week for the first week and weekly thereafter until 12 weeks after surgery.

2.5 Motor evoked potential measurements

Twelve weeks after surgery, six rats randomly selected from each group were anesthetized for measuring motor evoked potentials (MEPs) by MYTO electromyogram (ESAOTE, Italy) by blinded observers. The stimulating electrodes were placed on the cerebral cortex and the lower injury site (at about T11), and the recording electrode on the gastrocnemius muscle. The measurements were repeated three times for each site.

2.6 Retrograde axonal tracing

Twelve weeks after surgery, two rats randomly selected from each group were examined with Fluoro-Ruby (FR) retrograde axonal tracing. After rats were anaesthetized and fixed on a stereotaxic apparatus, the spinal cord was re-exposed at T10–11, and 6 μl of 10% FR solution (Chemicon International Inc, Temecula, CA) was injected at 1.0 mm bilaterally to the midline of spinal cord. After incision closure, the animals survived for 1 week to allow retrograde transport of tracer.

2.7 Histological and immunofluorescent analysis

Twelve weeks after surgery, the animals of different groups, including those had been subjected to retrograde tracing, were anesthetized, and transcardially perfused with pre-cooled 4% paraformaldehyde in 0.1 M phosphate buffer (PB, pH 7.2). After harvested and post-fixed, the spinal cord segment at rostral T7 and caudal T11 (for all rats) and the brain segment (for animals subjected to retrograde tracing) were sectioned on a cryostat (Leica, Heidelberg, Germany). The sections from two rats of each group were serially collected for three-dimensional reconstruction. As to other sections, every third section was mounted on gelatin-coated slides.

A portion of slices were subjected to hematoxylin–eosin (HE) and Nissl staining for histological observations. Another portion of slices were subjected to immunohistochemistry. They were allowed to incubate with primary antibodies, mouse-anti-NF (1:800, Sigma, St. Louis, MO) or rabbit-anti-GFAP (1:100, Sigma), at 4°C overnight. Secondary antibodies were TRITC conjugated goat-anti-mouse or goat-anti-rabbit IgG (1:256 or 1:80, Sigma), used for 2 h incubation at room temperature. Afterwards, the sections were coverslipped and observed under a fluorescence microscope (Leica, Wetzlar, Germany). These sections were observed by blinded observers.

2.8 Electron microscopy analysis

The spinal cord segments at T7–T11 were harvested from one rat randomly selected from BMSCs group and Chitosan group. They were fixed in 4% glutaraldehyde, and then post-fixed with 1% osmic acid, gradiently dehydrated with ethanol, embedded in epoxy resin, cut on the ultramicrotome (Leica, Heidelberg, Germany), stained by uranyl acetate–citric acid, and observed under a transmission electron microscope (JEOL Ltd., Tokyo, Japan) by blinded observers.

2.9 Three-dimensional (3D) reconstruction of regenerated tissues

Digital photomicrographs of pretreated spinal cord sections were obtained with a DFC 300FX color digital camera (Leica, Heidelberg, Germany) after HE staining. The resulting photomicrographs were colored with the software Photoshop CS 2.0 (Adobe, USA). In brief, the empty part was filled with red (Grey value: Red 255, Blue 0, Green 0), the remaining parts were filled with blue (Grey value: Red 0, Blue 255, Green 0), and the regenerated tissues in the empty part were filled with yellow (Grey value: Red 255, Blue 255, Green 0) as to increase the visual effects. Finally, three-dimensional reconstruction was carried out with the software 3D Doctor (Adobe, USA) to reveal the geometry of internal regenerated tissues.

2.10 Statistical analysis

The data of Basso, Beattie and Bresnahan (BBB) scores were analyzed by using repeated measures ANOVA with a

GraphPad Prism 4.0 software (GraphPad Software Inc., San Diego CA, USA) and the data of MEPs were expressed as means ± SEM and analyzed by using one-way ANOVA with a SPSS10.0 software package (SPSS Inc., Chicago, IL, USA). If there was a significant overall difference among groups, pair-wise comparisons were legitimately conducted by Fisher's least significant difference test. Values of $P < 0.05$ were considered statistically significant.

3 Results

3.1 Characterization of cultured BMSCs and physiochemical properties of chitosan conduits

At different passages, the isolated BMSCs grew rapidly and exhibited a spindle or polygon shape. Immunohistochemistry indicated that BMSCs expressed CD90, but not CD11b and CD 45, and immunostained cells numbered 79.19% of a whole cell population according to analysis by FACScan.

The morphology of chitosan conduits was observed by SEM. The dense outer layer of conduits ensured mechanical strength and also exerted a barrier function by preventing ingrowth of fibrous tissues, while the sponge-like inner layer of conduits could allow the exchange of nutrition and fluids (Fig. 1). SEM measurements further indicated the inner and outer diameter of 1.8 and 2.0 mm, respectively, for the conduit. The mechanical measurements indicate that the maximum fracture strength and compressive strength of the chitosan conduit are 164.5 ± 0.3 and 542.9 ± 0.8 N, respectively, under dry conditions, or 82.9 ± 0.4 and 49.0 ± 0.5 N, respectively, under wet conditions.

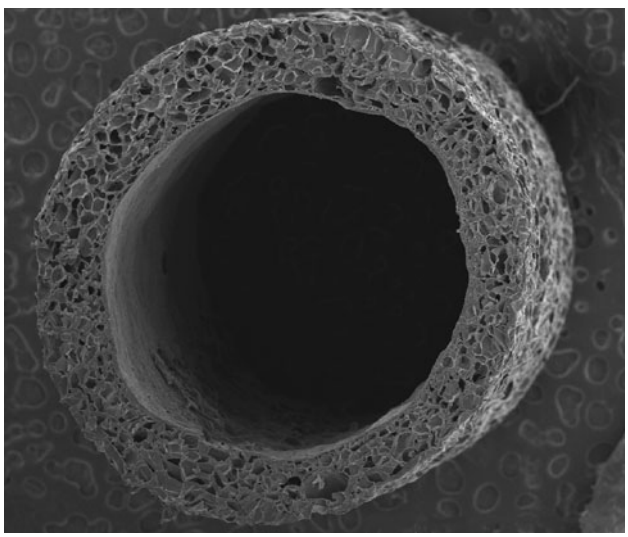

Fig. 1 Scanning electron micrograph of the chitosan conduit

3.2 Motor functional recovery

In this study, transection surgery to spinal cord resulted in paraplegia of two hindlimbs, so the BBB score in all animals was measured as 0 immediately after surgery (Table 1). Since 1 week after surgery BBB scores were changed in all groups. Statistical analysis showed that the BBB score of animals in BMSCs group was significantly higher than those in Unbridged group ($P < 0.01$) and Chitosan group ($P < 0.05$) (Fig. 2a).

3.3 Electrophysiological parameters

Twelve weeks after surgery, MEPs were recorded in BMSCs group and Chitosan group on stimulation either of the cerebral cortex or the lower injury site, but in Unbridged group, MEPs were recorded only on stimulation of the lower injury site and no MEPs recorded on stimulation of the cerebral cortex (Fig. 2b–d).

We compared the latency period and amplitude, respectively, of MEPs measured in different groups on stimulation of the cerebral cortex. The latency period in BMSCs group was significantly shorter than that in Chitosan group. And the amplitude in BMSCs group was significantly higher than that in Chitosan group (Fig. 2e, f).

On stimulation of the lower injury site, there was no statistically significant difference in the latency period among all groups. The amplitude in BMSCs group was significantly higher than that in Chitosan group or Unbridged group (Fig. 2g, h).

3.4 General observations of spinal cord

Twelve weeks after surgery, gross observation showed that accompanied with the partial degradation of chitosan conduits, the newly-regenerated tissue connected the stumps across the gap in the spinal cord, showing a complete anatomical structure, while Unbridged group showed no regenerated tissue between two stumps with the residual dura mater observed (Fig. 3).

3.5 Retrograde axonal tracing

Neurons labeled with red fluorescence were detected in the cerebral cortex 1 week after the injection of FR in all implanted groups. Most of the labeled neurons were spindle-shaped in Chitosan group and round in BMSCs group. Dense red fluorescence aggregated in the cytoplasm rather than the nuclei within the labeled neuron (Fig. 4).

Table 1 The BBB score for three different groups

	1 week	2 week	3 week	4 week	5 week	6 week	7 week	8 week	9 week	10 week	11 week	12 week
Unbridged group	1.9 ± 1.00	3.9 ± 0.66	5.6 ± 0.50	6.4 ± 0.74	7.3 ± 0.58	7.6 ± 0.51	7.6 ± 0.65	7.7 ± 0.42	7.8 ± 0.43	7.9 ± 0.73	7.9 ± 0.73	8.0 ± 0.78
Chitosan group	1.7 ± 0.83	3.6 ± 0.63	5.3 ± 0.95	7.3 ± 0.83**	7.6 ± 0.63	7.9 ± 0.66	7.9 ± 0.62	8.0 ± 0.55	8.3 ± 0.61*	8.4 ± 0.84*	8.5 ± 0.65*	8.5 ± 0.85*
BMSCs group	1.8 ± 0.58	4.9 ± 0.47**##	6.3 ± 0.83**##	7.2 ± 0.36**	7.4 ± 0.48	7.7 ± 0.47	8.0 ± 0.47	8.2 ± 0.43**	8.6 ± 0.63**	8.8 ± 0.87**#	8.9 ± 0.25**#	8.9 ± 0.73**#

** $P < 0.01$ versus Unbridged group, * $P < 0.05$ versus Unbridged group, ## $P < 0.01$ versus Chitosan group, # $P < 0.05$ versus Chitosan group

3.6 Histological evaluation

Twelve weeks after surgery, for BMSCs group and Chitosan group, HE staining of the transversely sectioned mid-portion of regenerated segments indicated that connective tissues enwrapped the partially degraded chitosan conduit, and the regenerated blood vessels and macrophages were observed in the regenerated region. Nissl-positive neurons were found at the regenerated segment for both implanted groups (Fig. 5). Unbridged group showed only residual spinal dura mater and scar tissue between two stumps of the gap.

To confirm that the regenerated tissues were nerve tissues, immunofluorescent double-staining was performed. For both implanted animals a number of NF-positive nerve fibers and neurons were detected at the distal and proximal stump of the injured spinal cord, and a few NF-positive nerve fibers and neurons were also found at the mid-portion of the regenerated tissue (Fig. 6).

3.7 Electron microscopic analysis

At 12 weeks after surgery, transmission electron microscopy of the mid-portion of the regenerated tissue showed that the regenerated tissue in Chitosan group mainly consisted of a large number of collagens and fibroblasts, while many regenerated myelination nerve fibers and newly-regenerated capillaries were observed in BMSCs group. Furthermore, the forming myelin sheath fibers in BMSCs group had a compact and uniform structure, including clear, higher electron density lamellar structure, but with few fibroblasts or collagen fibers (Fig. 7).

3.8 The 3D reconstruction of regenerated tissues

For animals in BMSCs group and Chitosan group, the digital photomicrographs derived from 3D reconstruction not only provided further evidence on nerve regeneration occurring at 12 weeks after implantation, but revealed that the volume of syringomyelia were reduced to some degrees. The volume of the cavities was smaller in BMSCs group than in Chitosan group (Fig. 8).

4 Discussion

Different therapeutic strategies have been developed for the repair of SCI [31–35]. The aim of this study was to determine whether implantation with BMSCs-loaded chitosan conduit following SCI could improve the microenvironment of the injured spinal cord and promote axonal regeneration and function restoration of the injured spinal

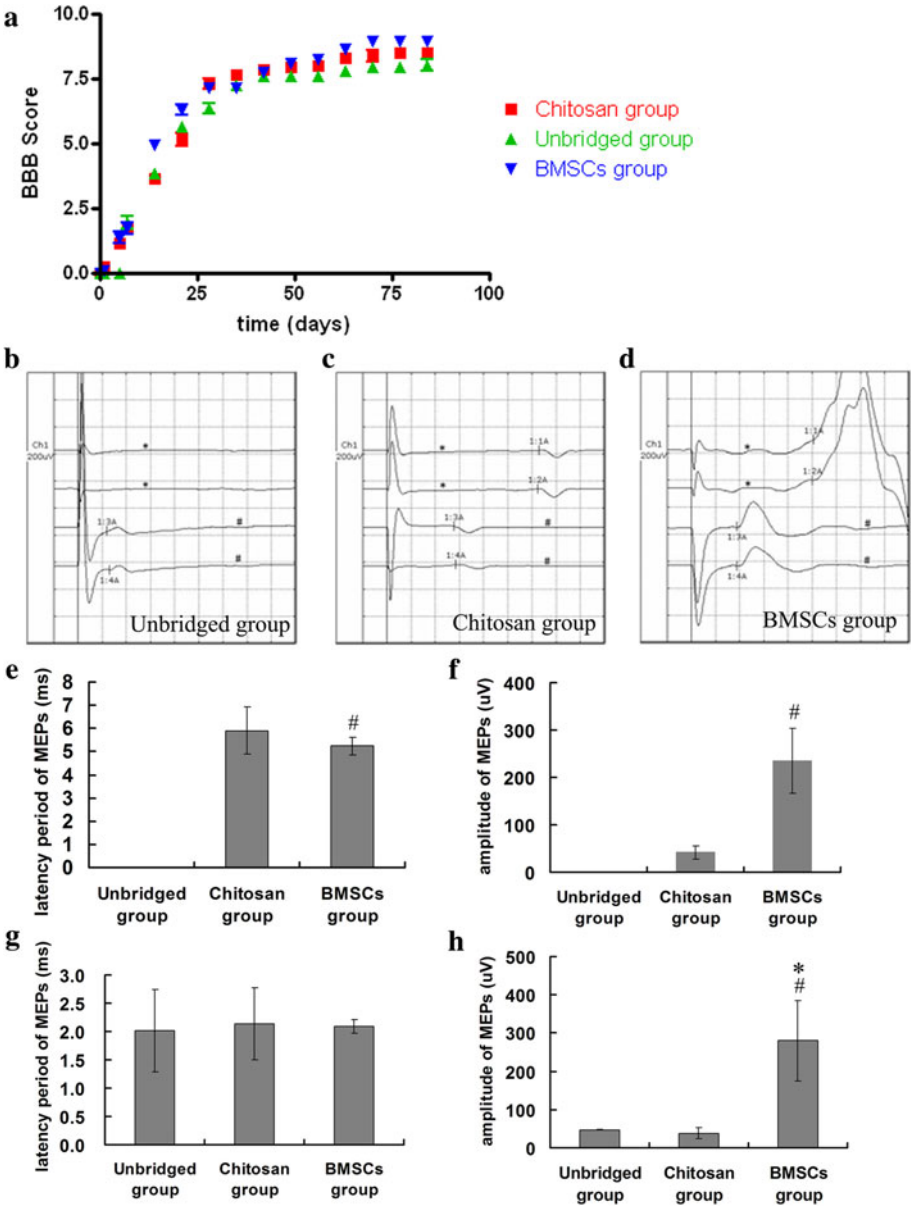

Fig. 2 **a** The time-dependent changes in the BBB score for three different groups. **b–d** The electromyograms showing MEPs recorded following stimulation of the cerebral cortex (marked with *) and the lower injury site (marked with #), respectively. It was noted that no MEPs were recorded when the cerebral cortex was stimulated in Unbridged group. The histograms showing the comparisons of the latency period and amplitude of MEPs recorded after stimulating the cerebral cortex (**e**, **f**) and the lower injury site (**g**, **h**), respectively. $^{\#}P < 0.05$ compared with Chitosan group; $^{*}P < 0.05$ compared with Unbridged group

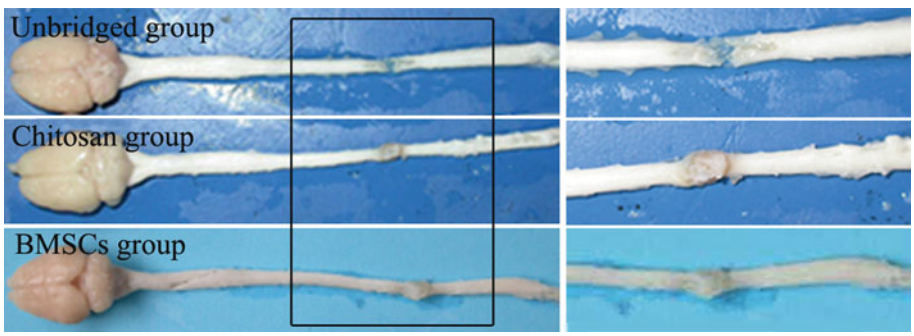

Fig. 3 Gross observation of spinal cord in three different groups (in the *left panel*) at 12 weeks after surgery. Also shown (in the *right panel*) are higher magnifications of the boxed areas

cord. As a conduit material, chitosan has many excellent properties that make it suitable for engineered nerve grafts [5, 36]. BMSCs are an ideal candidate to serve as cell implants because (1) they are easily isolated and propagated in vitro (2) they may be non-immunogenic in an autogeneic setting (3) they bypass many of the ethical concerns associated with use of embryonic stem cells in a clinical setting [22, 37]. Considering a good

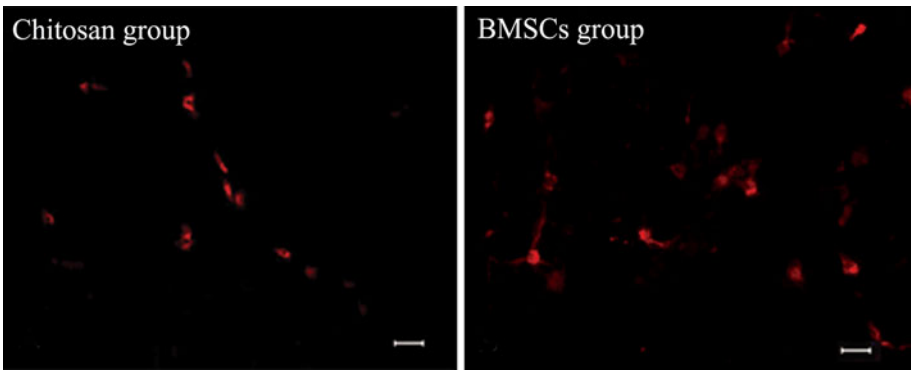

Fig. 4 Light micrographs indicating that neurons labeled with red fluorescence were detected in the cerebral cortex 1 week after the injection of FR in Chitosan group and BMSCs group, respectively. *Scale bar* 20 μm

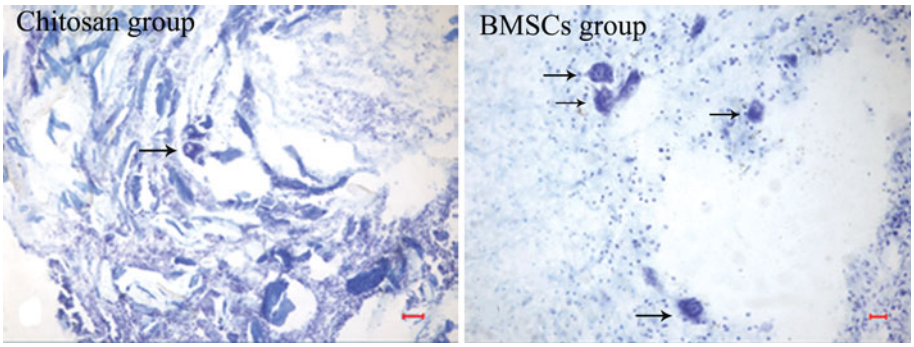

Fig. 5 Nissle staining for histological observations. Nissle-positive neurons (as indicated by *arrows*) were found at the regenerated segment for Chitosan group and BMSCs group 12 weeks after surgery. *Scale bar* 50 (Chitosan group) and 20 μm (BMSCs group), respectively

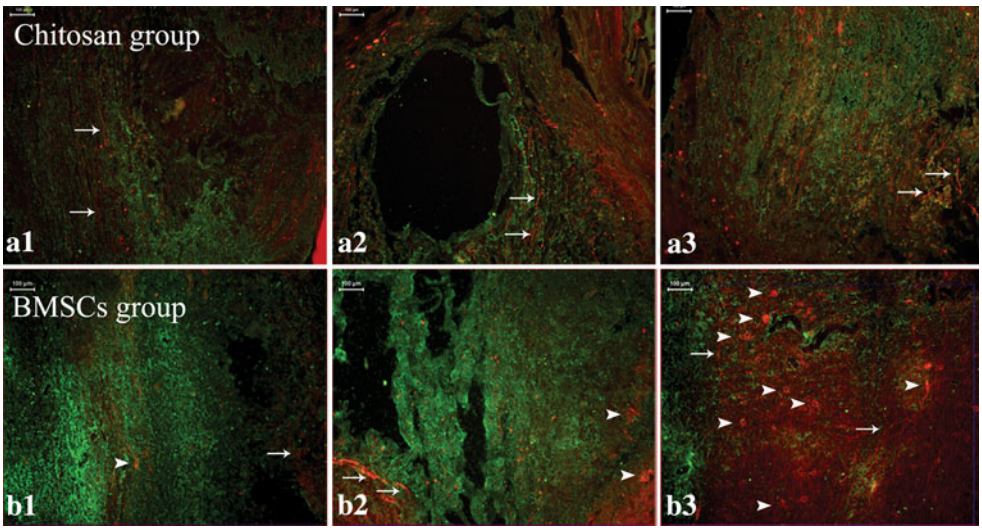

Fig. 6 Light micrographs following double-staining for NF (*red*) and GFAP (*green*) on the transversely sectioned proximal stump of the injured side (**a1**, **b1**), mid-portion of the regenerated tissue (**a2**, **b2**) and distal stump of the injured side (**a3**, **b3**) in Chitosan group (**a1**–**a3**), and BMSCs group (**b1**–**b3**), respectively. *Arrows* and *arrow heads* indicate NF-positive nerve fibers and neurons, respectively. *Scale bar* 100 μm (Color figure online)

biocompatibility of chitosan with BMSCs [38], we tried the joint use of chitosan conduits and BMSCs as nerve grafts to bridge the neural gap generated by SCI, and examined the feasibility of this new approach.

The BBB score was used to evaluate the functional recovery after SCI. The data indicated that the BMSCs-loaded chitosan conduit provided a better recovery in locomotor function as compared to the chitosan conduit without BMSCs. This result is consistent with that reported by previous studies, which claim that multipotential stem cells improve the condition of the microenvironment and promote motor function restoration of hindlimbs [14, 39]. As is known, even though the regenerated axons at the caudal end of the lesion area kept increasing, the increased number of regenerated axons could not necessarily establish functional connection with the host spinal cord [40],

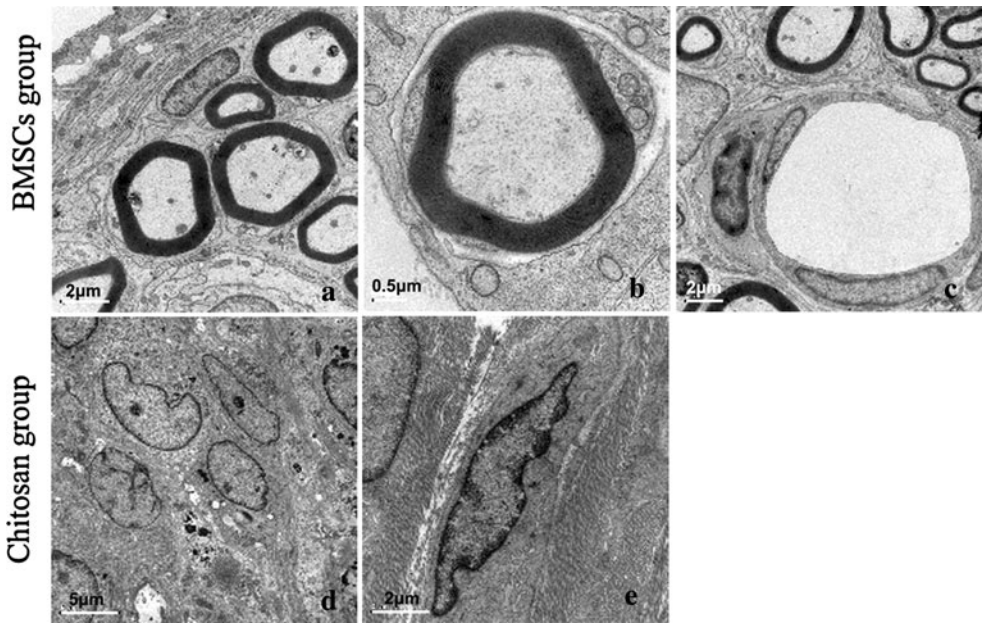

Fig. 7 Transmission electron micrographs of the mid-portion of the regenerated tissue in BMSCs group (**a**, **b**) and Chitosan group (**d**, **e**), respectively, from which many regenerated myelination nerve fibers and numerous new unmyelinated nerve fibers, could be compared among groups. Also shown in (**c**) is transmission electron micrograph of the newly-regenerated capillaries in BMSCs group. *Scale bar* 2 (**a**, **c**, and **e**), 0.5 (**b**) and 5 (**d**) μm, respectively

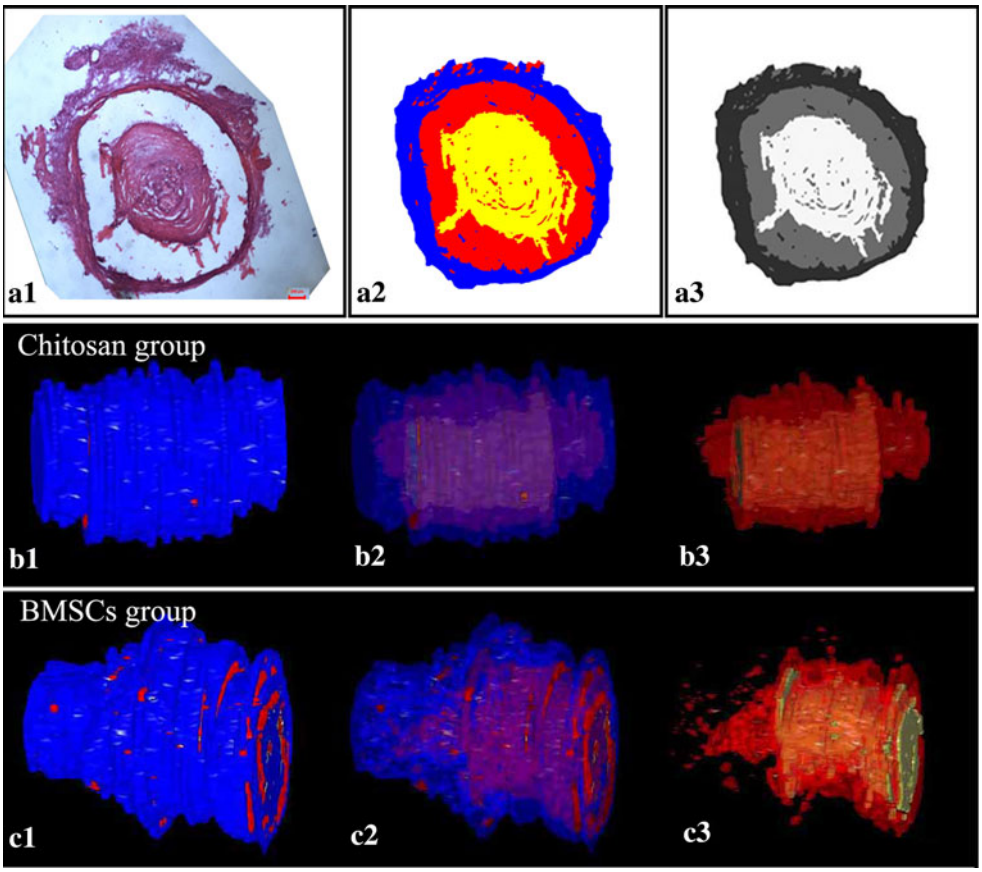

Fig. 8 The 3D reconstruction of the injured site obtained at 12 weeks after implantation with tissue engineered grafts. A flowchart (**a1**–**a3**) demonstrating the procedures of 3D reconstruction: step 1, registered images after HE staining (**a1**); step 2, semi-automatic segmentation by Photoshop software (**a2**); and step 3, segmentation of grey image by 3D Doctor software (**a3**). Digital photomicrographs, obtained by 3D reconstruction, showing the tissue regeneration and the cavity volume in Chitosan group (**b1**–**b3**), BMSCs group (**c1**–**c3**), respectively. The spinal cord cavity was shown in red color, the remaining parts surrounding out the cavities in *blue color*, and the regenerated tissues in *yellow color*. **b1**, **c1** the full view; **b2**, **c2** the scenograph; and **b3**, **c3** the view of cavities and the regenerated tissues. *Scale bar* 200 μm (Color figure online)

only stable and long-term regeneration of an anatomical structure is crucial for permanent functional recovery. Support cells including BMSCs may contribute to the formation of a complete anatomical structure.

The MEP parameters were better in BMSCs group than in Chitosan group. This suggested that a certain concentration of BMSCs was necessary for motor function restoration of spinal cord. FR retrograde tracing provided further evidence that the ascending tract had been regenerated in the adaptive environment and the neural path was established.

The traditional theory explains that the formation of glial scars is due to the aggregation of astrocyte, oligodendrocyte, macrophage, fibroblast, and other cells. In the injured spinal cord, the resultant glial scars would impede the migration of regenerated axons from one stump to the other [20, 21]. Histology showed that at 12 weeks after implantation a large amount of myelinated nerve fibers, unmyelinated nerve fibers, and blood vessels appeared in the injured lesion in BMSCs group. In contrast there were a limited number of nerve fibers but much more collagen fibers appearing in Chitosan group. These findings were similar to the results of NSCs implantation [16]. Immunofluorescent analysis showed that some NF-labeled neurons/nerve fibers formed in the injured lesion in BMSCs group.

As we know, the pathological processes for syringomyelia after SCI include the necrosis of the damaged nerve cells in the gray matter of spinal cord and the demyelination of nerve fibers in white matter followed by the formation of small cysts and their integration into cavities with different sizes. The resultant glial scars cause the contracture of the spinal cord stumps, which in turn increases the cavity volume. The 3D reconstruction analysis showed that implantation with either chitosan conduits alone or BMSCs-loaded chitosan conduits restore the continuity of the spinal cord and result in nerve regeneration within nerve grafts. The statistical analysis indicated that the volume of syringomyelia for BMSCs group was much smaller than that for Chitosan group. This result, in couple with electron microscopic observation, confirmed that addition of BMSCs to chitosan conduits led to a lower incidence of syringomyelia.

5 Conclusions

Our results presented here show that implantation of chitosan conduits filled with BMSCs across the transected gap in the spinal cord could promote axonal regeneration and myelination and cause a certain degree of functional recovery.

Acknowledgments This research was supported by grant from Natural Science Foundation of China, No. 30870643 and Project Funded by the Priority Academic Program Development of Jiangsu Higher Education Institutions. We thank Professor Jie Liu for assistance in manuscript preparation.

References

1. Willerth SM, Sakiyama-Elbert SE. Cell therapy for spinal cord regeneration. Adv Drug Deliv Rev. 2008;60(2):263–76.
2. He P, Davis SS, Illum L. In vitro evaluation of the mucoadhesive properties of chitosan microspheres. Int J Pharm. 1998;166(1):75–88.
3. Yang Y, Hu W, Wang X, Gu X. The controlling biodegradation of chitosan fibers by *N*-acetylation in vitro and in vivo. J Mater Sci Mater Med. 2007;18:2117–21.
4. Gan Q, Wang T, Cochrane C, McCarron P. Modulation of surface charge, particle size and morphological properties of chitosan-TPP nanoparticles intended for gene delivery. Colloids Surf B. 2005;44(2–3):65–73.
5. Cheng M, Cao W, Gao Y, Gong Y, Zhao N, Zhang X. Studies on nerve cell affinity of biodegradable modified chitosan films. J Biomater Sci Polym Ed. 2003;14(10):1155–67.
6. Yuan Y, Zhang P, Yang Y, Wang X, Gu X. The interaction of Schwann cells with chitosan membranes and fibres in vitro. Biomaterials. 2004;25(18):4273–8.
7. Scanga VI, Goraltchouk A, Nussaiba N, Shoichet MS, Morshead CM. Biomaterials for neural-tissue engineering—chitosan supports the survival, migration, and differentiation of adult-derived neural stem and progenitor cells. Can J Chem. 2010;88(3):277–87.
8. Cho Y, Shi RY, Borgens RB. Chitosan produces potent neuroprotection and physiological recovery following traumatic spinal cord injury. J Exp Biol. 2010;213(9):1513–20.
9. Yang YM, Liu M, Gu Y, Lin SY, Ding F, Gu XS. Effect of chitooligosaccharide on neuronal differentiation of PC-12 cells. Cell Biol Int. 2009;33(3):352–6.
10. Khodagholi F, Eftekharzadeh B, Maghsoudi N, Rezaei PF. Chitosan prevents oxidative stress-induced amyloid beta formation and cytotoxicity in NT2 neurons: involvement of transcription factors Nrf2 and NF-kappa β. Mol Cell Biochem. 2010;337(1–2):39–51.
11. Ogawa Y, Sawamoto K, Miyata T, Miyao S, Watanabe M, Nakamura M, Bregman BS, Koike M, Uchiyama Y, Toyama Y, Okano H. Transplantation of in vitro-expanded fetal neural progenitor cells results in neurogenesis and functional recovery after spinal cord contusion injury in adult rats. J Neurosci Res. 2002;69(6):925–33.
12. Kulbatski I, Mothe AJ, Nomura H, Tator CH. Endogenous and exogenous CNS derived stem/progenitor cell approaches for neurotrauma. Curr Drug Targets. 2005;6(1):111–26.
13. Novikova LN, Pettersson J, Brohlin M, Wiberg M, Novikov LN. Biodegradable poly-beta-hydroxybutyrate scaffold seeded with Schwann cells to promote spinal cord repair. Biomaterials. 2008;29(9):1198–206.
14. Olson HE, Rooney GE, Gross L, Nesbitt JJ, Galvin KE, Knight A, Chen B, Yaszemski MJ, Windebank AJ. Neural stem cell- and Schwann cell-loaded biodegradable polymer scaffolds support axonal regeneration in the transected spinal cord. Tissue Eng Part A. 2009;15(7):1797–805.
15. Steward O, Sharp K, Selvan G, Hadden A, Hofstadter M, Au E, Roskams J. A re-assessment of the consequences of delayed transplantation of olfactory lamina propria following complete spinal cord transection in rats. Exp Neurol. 2006;198(2):483–99.

16. Nomura H, Zahir T, Kim H, Katayama Y, Kulbatski I, Morshead CM, Shoichet MS, Tator CH. Extramedullary chitosan channels promote survival of transplanted neural stem and progenitor cells and create a tissue bridge after complete spinal cord transection. Tissue Eng Part A. 2008;14(5):649–65.
17. Tohill M, Mantovani C, Wiberg M, Terenghi G. Rat bone marrow mesenchymal stem cells express glial markers and stimulate nerve regeneration. Neurosci Lett. 2004;362(3):200–3.
18. Jin K, Mao XO, Batteur S, Sun Y, Greenberg DA. Induction of neuronal markers in bone marrow cells: differential effects of growth factors and patterns of intracellular expression. Exp Neurol. 2003;184(1):78–89.
19. Woodbury D, Schwarz EJ, Prockop DJ, Black IB. Adult rat and human bone marrow stromal cells differentiate into neurons. J Neurosci Res. 2000;61(4):364–70.
20. Kopen GC, Prockop DJ, Phinney DG. Marrow stromal cells migrate throughout forebrain and cerebellum, and they differentiate into astrocytes after injection into neonatal mouse brains. Proc Natl Acad Sci USA. 1999;96(19):10711–6.
21. Ankeny DP, McTigue DM, Jakeman LB. Bone marrow transplants provide tissue protection and directional guidance for axons after contusive spinal cord injury in rats. Exp Neurol. 2004; 190(1):17–31.
22. Rooney GE, McMahon SS, Ritter T, Garcia Y, Moran C, Madigan NN, Flügel A, Dockery P, O'Brien T, Howard L, Windebank AJ, Barry FP. Neurotrophic factor-expressing mesenchymal stem cells survive transplantation into the contused spinal cord without differentiating into neural cells. Tissue Eng Part A. 2009;15(10): 3049–59.
23. Vaquero J, Zurita M, Oya S, Santos M. Cell therapy using bone marrow stromal cells in chronic paraplegic rats: systemic or local administration? Neurosci Lett. 2006;398(1–2):129–34.
24. Zurita M, Vaquero J. Bone marrow stromal cells can achieve cure of chronic paraplegic rats: functional and morphological outcome one year after transplantation. Neurosci Lett. 2006;402(1–2):51–6.
25. Ishikawa N, Suzuki Y, Dezawa M, Kataoka K, Ohta M, Cho H, Ide C. Peripheral nerve regeneration by transplantation of BMSC-derived Schwann cells as chitosan gel sponge scaffolds. J Biomed Mater Res A. 2009;89(4):1118–24.
26. Chen X, Wang XD, Chen G, Lin WW, Yao J, Gu XS. Study of in vivo differentiation of rat bone marrow stromal cells into Schwann cell-like cells. Microsurgery. 2006;26(2):111–5.
27. Lin W, Chen X, Wang X, Liu J, Gu X. Adult rat bone marrow stromal cells differentiate into Schwann cell-like cells in vitro. In Vitro Cell Dev Biol Anim. 2008;44(1–2):31–40.
28. Wang X, Hu W, Cao Y, Yao J, Wu J, Gu X. Dog sciatic nerve regeneration across a 30-mm defect bridged by a chitosan/PGA artificial nerve graft. Brain. 2005;128(8):1897–910.
29. Basso DM, Beattie MS, Bresnahan JC. A sensitive and reliable locomotor rating scale for open field testing in rats. J Neurotrauma. 1995;12(1):1–21.
30. Onifer SM, Rabchevsky AG, Scheff SW. Rat models of traumatic spinal cord injury to assess motor recovery. ILAR J. 2007; 48(4):385–95.
31. David S, Lacroix S. Molecular approaches to spinal cord repair. Annu Rev Neurosci. 2003;26:411–40.
32. Kakulas BA. Neuropathology: the foundation for new treatments in spinal cord injury. Spinal Cord. 2004;42(10):549–63.
33. Syková E, Jendelová P, Urdzíková L, Lesný P, Hejcl A. Bone marrow stem cells and polymer hydrogels—two strategies for spinal cord injury repair. Cell Mol Neurobiol. 2006;26(7–8):1113–29.
34. Hejcl A, Lesný P, Prádný M, Michálek J, Jendelová P, Stulík J, Syková E. Biocompatible hydrogels in spinal cord injury repair. Physiol Res. 2008;57(3 Suppl):S121–32. Epub 2008 May 13. Review.
35. Busch SA, Horn KP, Cuascut FX, Hawthorne AL, Bai L, Miller RH, Silver J. Adult NG^{2+} cells are permissive to neurite outgrowth and stabilize sensory axons during macrophage-induced axonal dieback after spinal cord injury. J Neurosci. 2010;30(1): 255–65.
36. Itoh S, Suzuki M, Yamaguchi I, Takakuda K, Kobayashi H, Shinomiya K, Tanaka J. Development of a nerve scaffold using a tendon chitosan tube. Artif Organs. 2003;27(12):1079–88.
37. Barry FP, Murphy JM, English K, Mahon BP. Immunogenicity of adult mesenchymal stem cells: lessons from the fetal allograft. Stem Cells Dev. 2005;14(3):252–65.
38. Moreau JL, Xu HH. Mesenchymal stem cell proliferation and differentiation on an injectable calcium phosphate-chitosan composite scaffold. Biomaterials. 2009;30(14):2675–82.
39. Zhang J, Li Y, Lu M, Cui Y, Chen J, Noffsinger L, Elias SB, Chopp M. Bone marrow stromal cells reduce axonal loss in experimental autoimmune encephalomyelitis mice. J Neurosci Res. 2006;84(3):587–95.
40. Li X, Yang Z, Zhang A, Wang T, Chen W. Repair of thoracic spinal cord injury by chitosan tube implantation in adult rats. Biomaterials. 2009;30(6):1121–32.